J|A|C|S
ARTICLES
Published on Web 03/06/2007

Chiral Separation: Mechanism Modeling in Two-Dimensional Systems

Irina Paci,*,† Igal Szleifer,‡ and Mark A. Ratner†

Contribution from the Department of Chemistry and Materials Research Center, Northwestern University, Evanston, Illinois, 60208, and Department of Chemistry, Purdue University, West Lafayette, Indiana, 47907

Received September 5, 2006; E-mail: ipaci@chem.northwestern.edu

Abstract: Fluid phase separations of racemates are difficult because the subtle, short-ranged differences in intermolecular interactions of like and unlike pairs of chiral molecules are typically smaller than the thermal energy. A surface restricts the configurational space available to the pair of interacting molecules, thus changing the effective interactions between them. Because of this restriction, a surface can promote chiral separation of mixtures that are racemic in bulk. In this paper, we investigate chiral symmetry breaking induced by an achiral surface in a racemate. A parallel tempering Monte Carlo algorithm with tempering over the temperature domain is used to examine the interplay between molecular geometry and energetics in promoting chiral separations. The system is restricted to evolve in two dimensions. By controlling the balance between electrostatic and steric interactions, one can direct the surface assembly of the chiral molecules toward formation of small clusters of identical molecules. When molecular shape asymmetry is complemented by dipolar alignment, chiral micellar clusters of like molecules are assembled on the surface. We examine the case of small model molecules for which the two-dimensional restriction of the pair potential is sufficient to induce chiral segregation. An increase in molecular complexity can change the balance of intermolecular interactions to the point that heterochiral pairs are energetically more favored. In this case, we find conditions in which formation of homochiral micelles is still achieved, due to a combination of multibody and entropic effects. In such systems, an examination of the pair potential alone is insufficient to predict whether the multimolecular racemate will or will not segregate.

1. Introduction

Chiral symmetry breaking is the process by which an achiral phase is resolved into two enantiomeric domains. This refers not only to the separation of a homogeneous racemic mixture but also to induced chiral separations, in which an achiral phase becomes chiral either on a surface or after being exposed to a chiral precursor to preferentially align the phase. Spontaneous chiral resolution of racemates during crystallization, although made famous by the experiment of Louis Pasteur on sodium ammonium tartrate, is rare (only 5−10% of organic racemates exhibit this property[1]). Chiral resolution has since been the subject of numerous studies. Besides its direct application as a separative method, spontaneous resolution is intimately related to the process of chiral recognition, in general. Thus, its understanding and control are not only important in understanding physiological processes but also in drug design and manufacturing.[2−10] Some drugs are only effective in a given enantiomeric form, so the racemic drug can be considered 50% impure.[11,12] In some cases, whereas one enantiomer is an active drug agent, the other is toxic.[13] If present, the preference of one molecule for its twin rather than its enantiomer is short ranged. When separation is attempted from a fluid phase, these preferences are most likely lost through rotational averaging or overwhelmed by thermal motion.[12,14−16] This makes chiral separations from such phases difficult, in general. Breaking the symmetry of the phase by using a surface has the potential to reduce these effects, the separation of homochiral domains upon adsorption having been observed experimentally.[17−24]

† Northwestern University.
‡ Purdue University.

(1) Wei, Y.; Kannappan, K.; Flynn, G. W.; Zimmt, M. B. *J. Am. Chem. Soc.* **2004**, *126*, 5318.
(2) Stinson, S. C. *C & E News* **2001**, *79*, 35.
(3) Thayer, A. M. *C & E News* **2002**, *80*, 25.
(4) Rouhi, A. M. *C & E News* **2002**, *80*, 43.
(5) Hyun, M. H.; Ryoo, J.-J.; Pirkle, W. H. *J. Chromatogr. A* **2000**, *886*, 47.
(6) Pirkle, W. H.; Gan, K. Z.; Brice, L. J. *Tetrahedron: Asymmetry* **1996**, *7*, 2814.
(7) Pirkle, W. H.; Liu, Y. *J. Chromatogr. A* **1996**, *749*, 19.
(8) Topiol, S. *Chirality* **1989**, *1*, 69.
(9) Garten, S.; Biedermann, P. U.; Agranat, I.; Topiol, S. *Chirality* **2005**, *17*, S159.
(10) Perez-Garcia, L.; Amabilino, D. B. *Chem. Soc. Rev.* **2002**, *31*, 342.
(11) Seri-Levy, A.; West, S.; Richards, W. G. *J. Med. Chem.* **1994**, *37*, 1727.
(12) Craig, D. P.; Mellor, D. P. *Top. Curr. Chem.* **1976**, *63*, 1.
(13) Ahuja, S. *Chiral Separations: Applications and Technology*; American Chemical Society: Washington D. C., 1997.
(14) Paci, I.; Cann, N. M. *J. Chem. Phys.* **2001**, *115*, 8489.
(15) Craig, D. P.; Schipper, P. E. *Proc. R. Soc. Lond. A* **1975**, *342*, 19.
(16) Mason, S. F. *Optical Activity and Chiral Discrimination*; D. Reidel Publishing: The Netherlands, 1979.
(17) Humblot, V.; Barlow, S. M.; Raval, R. *Prog. Surf. Sci.* **2004**, *76*, 1.
(18) Jonkheijm, P.; Miura, A.; Zdanowska, M.; Hoeben, F. J. M.; de Feyter, S.; Schenning, A. P. H. J.; de Schryver, F. C.; Meijer, E. W. *Angew. Chem., Int. Ed.* **2004**, *43*, 74.
(19) Kühnle, A.; Linderoth, T. R.; Besenbacher, F. *J. Am. Chem. Soc.* **2003**, *125*, 14680.
(20) Spillmann, H.; Dmitriev, A.; Lin, N.; Messina, P.; Barth, J. V.; Kern, K. *J. Am. Chem. Soc.* **2003**, *125*, 10725.

Surfaces can aid in chiral resolutions in a number of ways. Chiral stationary phases have been used in high-performance liquid chromatography and gas chromatography for many years now.[5−7,25] In chiral chromatography, diastereomeric interactions are generated between the chiral stationary phase and one of the enantiomers to be separated. On the other hand, when chiral solvents are used, diastereomeric solvent−analyte pairs can be separated chromatographically on achiral columns.[26,27]

Recently, adsorption on achiral surfaces has been used to induce chiral symmetry breaking without formation of diastereomeric pairs.[19,21,22,24,28,29] Achiral surfaces can be used directly to limit, by adsorption, the configurational space available to the racemate to two dimensions. Both two-body and multibody potentials are changed as a consequence. Chiral recognition can then occur in systems that are racemic in three dimensions, by preferential alignment of groups of particles, facilitated by the surface. In this case, chiral domains of the pure enantiomers may form on the surface. A solid substrate can also induce chiral symmetry breaking in achiral adsorbates that become chiral when adsorbed. This achiral compound, once bound to the substrate, can form chiral domains. The surface thus patterned can be used as a low-cost chiral resolution catalyst.[1,17,20,23,24,30−39]

Chiral resolution from racemates has been achieved experimentally at a surface. A chiral amphiphilic tetracyclic alcohol was seen to separate in mirror-image domains at the aqueous surface by Eckhardt et al.[21] Walba et al.[22] obtained enantiomorphous domains when placing a racemic liquid crystal of a biphenylbenzoate on highly oriented pyrolytic graphite (HOPG). Similarly, Flynn and co-workers[23,24,40] obtained homochiral domains of 2-bromo-hexadecanoic acid of 30−100 nm width, when the racemate was adsorbed on HOPG. Jonkheijm et al.[18] observed chiral hexameric rosette clusters of oligo-(*p*-phenylenevinylene) on a surface during synthesis of rosette nanotubes. The rosette clusters had opposite "rotation" directions for enantiomers of different molecular lengths. Chiral clusters were also obtained on surfaces from heptahelicene[28] and tartaric acid.[41,42] Of direct interest to this investigation are two additional experimental results: the self-assembly of homochiral nanoclusters from a cysteine racemate on gold surfaces[19] and the self-assembly of homochiral supramolecular structures of rubrene on gold surfaces.[29] These experiments are two-dimensional analogues of Pasteur's aggregate formation. Although chiral chromatography and asymmetric synthesis are the methods of choice for process scale separations, spontaneous chiral resolution has been shown to be useful in a number of ways, particularly when the formation and separation of diastereomers is unsuitable.[1,25,43,44] In one method, chiral aggregates can be used as seeds in the spontaneous and separate crystallization from supersaturated racemic solutions. Another method uses chiral seeds of one of the enantiomers, obtained through spontaneous resolution, for separations by entrainment. Finally, chiral clusters formed by adsorption can interact stereospecifically to form large homochiral domains through multi-level supramolecular chiral assembly, as observed experimentally for rubrene.[29] The process holds promise for direct separation of enantiomers at the laboratory scale.

There are also experimental studies in which surfaces were patterned by chiral symmetry breaking in achiral adsorbates and then used for chiral separations. For example, Flynn and coworkers have used the achiral hexadecanoic acid, which, coadsorbed with racemic 2-bromo-hexadecanoic acid, leads to the formation of extended homochiral domains.[23] Relative configurations of the enantiomers are changed significantly in the presence of the achiral coadsorbate.

Given the general interest in chiral separations, particularly in direct symmetry breaking in two-dimensional systems, theoretical investigations can be important to understand the underlying physical origin of chiral resolutions on surfaces. Andelman and Orland[45] have already investigated the influence of the two-dimensional restriction on the free energy and potential energy of a pair of molecules. For the tripodal models the authors investigated, heterochiral pairs were more stable than homochiral pairs, both in two and three dimensions, although the difference was smaller in the two-dimensional pair interactions. The authors did not go on to examine what happens when a multimolecular monolayer is considered. As we will show below, examination of pair potentials is often insufficient to predict the behavior of the multimolecular system, and systems characterized by lower heterochiral pair potentials can still assemble in homochiral aggregates because of multibody interactions and entropic effects.

Molecular dynamics and periodic density functional theory simulations have previously been employed to understand the experimental results of chiral assembly on surfaces.[38,39,46,47] Such simulations are valuable for the specific systems being investigated, and their success depends on using good initial configurations for the assembled geometry. The configurations are inferred from the experimentally observed structures, and

(21) Eckhardt, C. J.; Peachey, N. M.; Swanson, D. R.; Takacs, J. M.; Khan, M. A.; Gong, X.; Kim, J.-H.; Wang, J.; Uphaus, R. A. *Nature* **1993**, *362*, 614.
(22) Stevens, F.; Dyer, D. J.; Walba, D. M. *Angew. Chem., Int. Ed. Engl.* **1996**, *35*, 900.
(23) Yablon, D. G.; Giancarlo, L. C.; Flynn, G. W. *J. Phys. Chem. B* **2000**, *104*, 7627.
(24) Yablon, D. G.; Wintgens, D.; Flynn, G. W. *J. Phys. Chem. B* **2002**, *106*, 5470.
(25) Jacques, J.; Collet, A.; Wilen, S. H. *Enantiomers, Racemates and Resolutions*; Wiley: New York, 1981.
(26) Martens, J.; Bhushan, R. *J. Liq. Chromatogr.* **1992**, *15*, 1.
(27) Lelievre, F.; Yan, C.; Zare, R. N.; Gareil, P. *J. Chromatogr. A* **1996**, *723*, 145.
(28) Fasel, R.; Parschau, M.; Ernst, K.-H. *Angew. Chem., Int. Ed.* **2003**, *42*, 5178.
(29) Blum, M.-C.; Cavar, E.; Pivetta, M.; Patthey, F.; Schneider, W.-D. *Angew. Chem., Int. Ed.* **2005**, *44*, 5334.
(30) Viswanathan, R.; Zasadzinski, J. A.; Schwartz, D. K. *Nature* **1994**, *368*, 440.
(31) Switzer, J. A.; Kothari, H. M.; Poizot, P.; Nakanishi, S.; Bohannan, E. W. *Nature* **2003**, *425*, 490.
(32) Kim, B.-I.; Cai, C.; Deng, X.; Perry, S. S. *Surf. Sci* **2003**, *538*, 45.
(33) Chen, Q.; Frankel, D. J.; Richardson, N. V. *Surf. Sci* **2002**, *497*, 37.
(34) Barlow, S. M.; Raval, R. *Surf. Sci. Rep.* **2003**, *50*, 201.
(35) Böhringer, M.; Morgenstern, K.; Schneider, W.-D.; Berndt, R.; Mauri, F.; de Vita, A.; Car, R. *Phys. Rev. Lett.* **1999**, *83*, 324.
(36) France, C. B.; Parkinson, B. A. *J. Am. Chem. Soc.* **2003**, *125*, 12712.
(37) Vidal, F.; Delvigne, E.; Stepanow, S.; Lin, N.; Barth, J. V.; Kern, K. *J. Am. Chem. Soc.* **2005**, *127*, 10101.
(38) Barth, J. V.; Weckesser, J.; Trimarchi, G.; Vladimirova, M.; de Vita, A.; Cai, C.; Brune, H.; Günter, P.; Kern, K. *J. Am. Chem. Soc.* **2002**, *124*, 7991.
(39) Böhringer, M.; Morgenstern, K.; Schneider, W.-D.; Berndt, R. *Angew. Chem., Int. Ed.* **1999**, *38*, 821.
(40) Fang, H.; Giancarlo, L. C.; Flynn, G. W. *J. Phys. Chem. B* **1998**, *102*, 7311.
(41) Lorenzo, M. O.; Baddeley, C. J.; Muryn, C.; Raval, R. *Nature* **2000**, *404*, 376.
(42) Humblot, V.; Haq, S.; Muryn, C.; Hofer, W. A.; Raval, R. *J. Am. Chem. Soc.* **2002**, *124*, 7991.
(43) Tissot, O.; Gouygou, M.; Dallemer, F.; Daran, J.-C.; Balavoine, G. G. A. *Angew. Chem., Int. Ed.* **2001**, *40*, 1076.
(44) Kostyanovsky, R. G.; Torbeev, V. Y.; Lyssenko, K. A. *Tetrahedron: Asymmetry* **2001**, *12*, 2721.
(45) Andelman, D.; Orland, H. *J. Am. Chem. Soc.* **1993**, *115*, 12322.
(46) Barbosa, L. A. M. M.; Sautet, P. *J. Am. Chem. Soc.* **2001**, *123*, 6639.
(47) Hermese, C. G. M.; van Bavel, A. P.; Jansen, A. P. J.; Barbosa, L. A. M. M.; Sautet, P.; van Santen, R. A. *J. Phys. Chem. B* **2004**, *108*, 11035.

change only locally during the simulation. Of particular theoretical interest have been liquid crystals of banana-shaped and related ("bent-core"[48]) molecules, achiral in three dimensions, which form two-dimensional chiral aggregates in their liquid crystal alignment.[48−51]

It should be emphasized that in two-dimensional as well as in three-dimensional systems, the presence and extent of chiral recognition is not a simple consequence of molecular asymmetry. It is the outcome of intermolecular and, for separations on surfaces, molecule−substrate interactions specific to the individual chiral compound. In a classical description, intermolecular interactions are comprised of a short-range repulsion part that ensures that molecules do not overlap, an attractive component that is due to van der Waals dispersion, and electrostatic terms describing the interaction of groups possessing partial or full charges. Formation of locally chiral structures occurs by preferential orientation of the molecules, according to these interactions. For example, hydrogen bonds, an electrostatic component, may promote a specific alignment for a set of molecules. Steric interactions, in the sense of the combination of repulsive and dispersive forces that describe the topological arrangement of atoms in the molecule, may promote alignment for like molecules but inhibit it for unlike molecules. The classical example of a glove matching a hand is encompassed in this type of recognition. The opposite effect is also possible. Here and in the following pages, we describe groups of particles or thermodynamic quantities as "like" if they refer to molecules of identical chirality, and "unlike" if they refer to different enantiomers.

In this article, Monte Carlo simulations are used to investigate chiral separations. We attempt to observe the assembly process when the molecules are allowed to evolve through molecular translation and rotation, reaching equilibrium structures independent of the choice of initial configurations. Further, we attempt to establish relationships among molecular structure, energetics, and the extent of separation using simple models. To explore these effects at a detailed level, while at the same time accounting for the collective assembly of relatively large numbers of molecules, we examine intermediate-size racemic systems, of 60−200 molecules.

Equilibrium structures formed by the racemates on the surface, and the conditions in which these structures are separated in enantiomorphic domains, are considered here. To limit the complexity of the problem and to directly examine variables of interest such as molecular morphology, the substrate is considered simply by restricting the racemate to evolve in two dimensions, rather than through specific molecule−surface interactions. The symmetry breaking effect of the surface, as opposed to the intrinsic chirality of the system, is examined by comparisons of two-dimensional results with calculations in which the molecules are allowed to evolve in three dimensions. Small five- to seven-atom chiral model molecules are used to understand how an increase in molecular complexity and the resulting pair interactions modify the self-assembly mechanism. Enantiospecific clustering results from both steric and electrostatic components of the intermolecular potential. The resulting structural building blocks are either small clusters of like molecules or double-chain heterochiral aggregates. We investigate the circumstances in which chiral clustering and separation are achieved when the system is restricted to two dimensions and how molecular structure and energetic factors impact the quality of this resolution. We find that by controlling the balance between the electrostatic and steric interactions on one hand, and between potential and entropic factors on the other, one can direct the assembly of chiral molecules on the surface.

Details of the Monte Carlo methodology, of the molecular models and measures of chiral segregation, are given in Section 2. Results for small five-atom molecules, and for larger molecules with more complicated pair potentials, are presented in Section 3. Our conclusions are outlined in the final section.

2. Method

2.1. Parallel Tempering Monte Carlo Methodology. Several modern methods in computer simulations overcome trapping in metastable configurations. Parallel tempering Monte Carlo (PTMC) is one such method, shown to work well for simulations of clusters,[52−55] because of its inherent ergodicity. Briefly, replicas of the system are simultaneously equilibrated at different temperatures, using canonical (constant number of particles, volume, and temperature) Monte Carlo moves. Ergodicity is sought by periodically performing configurational swaps between replicas with neighboring temperatures.

Simulations consist of a Markov chain of the following types of moves:

(i) Standard MC translational moves, based on the standard Metropolis acceptance criterion: for the canonical ensemble,

$$acc(o \rightarrow n) = \min\{1, \exp[-\beta(U(n) - U(o))]\} \qquad (1)$$

where $acc(o \rightarrow n)$ indicates the acceptance probability of a move from o to n, U is the total potential energy, n and o denote the "new" and "old" configurations, respectively, and $\beta = 1/k_B T$ is the inverse temperature.

(ii) Swap moves: two differing-temperature replicas of the system, i and $j = i + 1$, are randomly selected, and their configurations are swapped, with the acceptance probability given by:

$$acc(o \rightarrow n) = \min\{1, \exp[\Delta\beta \Delta U]\} \qquad (2)$$

where $\Delta\beta = \beta_i - \beta_j$ is the difference between the two neighboring inverse temperatures for which configurations are being swapped, and $\Delta U = U(x_i) - U(x_j)$ is the difference in energy between the two configurations.

Using this methodology, replicas evolving at high temperatures are able to sample regions of the potential energy surface that cannot be easily achieved directly at low temperatures. Through configurational exchanges, these regions are made available to lower temperature replicas as well. As a result, a replica that may have been trapped in a local minimum can be brought out via a configurational exchange. In addition, successive configurations sampled by one replica may become less correlated, and thus, each replica may achieve its equilibrium configuration much faster than without configuration swaps.[56] This convergence speed-up usually offsets the overhead due to the necessity of simulating multiple copies.

(48) Xu, J.; Selinger, R. L. B.; Selinger, J. V.; Shashidhar, R. *J. Chem. Phys.* **2001**, *115*, 4333.
(49) Selinger, J. V.; Wang, Z.-G.; Bruinsma, R. F.; Knobler, C. M. *Phys. Rev. Lett.* **1993**, *70*, 1139.
(50) Kohl, P. B.; Patrick, D. L. *J. Phys. Chem. B* **2001**, *105*, 8203.
(51) Yoneya, M.; Yokoyama, H. *J. Chem. Phys.* **2001**, *114*, 9532.
(52) Frantz, D. D. *J. Chem. Phys.* **2001**, *115*, 6136.
(53) Neirotti, J. P.; Calvo, F.; Freeman, D. L.; Doll, J. D. *J. Chem. Phys.* **2000**, *112*, 10340.
(54) Frenkel, D.; Smit, B. *Understanding Molecular Simulation From Algorithms to Applications*; Academic Press: San Diego, CA, 2002.
(55) Paci, I.; Szleifer, I.; Ratner, M. A. *J. Phys. Chem. B* **2005**, *109*, 12935.
(56) Hansmann, U. H. E. *Chem. Phys. Lett.* **1997**, *281*, 140.

The temperature range for parallel tempering is selected so that the minimum temperature corresponds to a compact assembly of the molecules (solid phase) whereas the highest temperature allows overcoming most energy barriers. To determine the temperature spacing between neighboring replicas and the number of replicas, trial runs are performed initially for each new system being investigated. Energy histograms are calculated for each temperature. The acceptance probability of replica swaps is predicted by the amount of overlap between two neighboring histograms. The larger the overlap, the more exchange attempts will be accepted. As a rule of thumb, about a 10% acceptance of exchange attempts is required for the parallel tempering method to work.[57] In this study, we used, for each calculation, 30−40 replicas evolving at different reduced temperatures, from 0.05 to 4.5 or 5.0 (see definition of reduced temperatures below). In the production runs, approximately 2×10^9 MC steps were carried out for each system. Here, a MC step is defined as one attempted particle move or configurational swap. Additional moves were performed as necessary to ensure convergence of the total energy for each replica. One to five percent of the moves were temperature swaps.

The molecules were restrained to move within a plane. Specifically, if the *z* axis is normal to this plane, molecules were allowed to translate within the plane and rotate around the *z* axis. Rotations around the *x* and *y* axes were not considered. At high density, constraining the molecular motion to two dimensions limits the amount of space each molecule can sample. In other words, moves that correspond to desorption−adsorption and diffusion in an experimental setup are not well represented. This restricts the ability of the system to reach the minimum energy configuration. Consequently, a third type of move was added to the Markov chain in the case of two-dimensional simulations:

(iii) Swaps between the positions of pairs of non-identical molecules (enantiomers). These molecular swaps were attempted, overall, in about (100/*N*)% of the moves (where *N* is the number of molecules in the sample) and accepted according to their Boltzmann factors.

2.2. Models, Intermolecular Potentials, and Chiral Segregation Measures. The racemates are composed of 60−200 rigid molecules, in a simulation box, with no periodic boundary conditions. The size of the simulation box is large enough that it does not impact the density of the resulting structures at the temperatures of interest here. Evaporative events (particles leaving the simulation box) are forbidden by simply rejecting moves that lead to evaporation. Intermolecular interactions are described with pairwise atom-based Lennard-Jones and electrostatic potentials:

$$U_{ab} = \sum_{i,j=1}^{n_{at}} \left[4\epsilon_{ij} \left(\left(\frac{\sigma_{ij}}{r_{ij}} \right)^{12} - \left(\frac{\sigma_{ij}}{r_{ij}} \right)^{6} \right) + \frac{q_i q_j e^2}{4\pi\epsilon_0 r_{ij}} \right] \quad (3)$$

where *a* and *b* denote two interacting molecules, n_{at} is the number of atoms in a molecule, ϵ_{ij} and σ_{ij} are the Lennard-Jones depth and distance parameters for atoms *i* and *j*, r_{ij} is the distance between the centers of the two atoms, q_i is the partial charge on atom *i*, *e* is the electronic charge, and ϵ_0 is the dielectric constant of vacuum. Mixed Lennard-Jones parameters are obtained using the Lorentz−Berthelot mixing rules: $\sigma_{ij} = (\sigma_{ii} + \sigma_{jj})/2$, $\epsilon_{ij} = \sqrt{\epsilon_{ii}\epsilon_{jj}}$. Molecules are considered rigid. We present in Figure 1 a sketch of one of the enantiomers for each of the systems considered here. The geometry and interaction parameters are given in Table 1. We used capital letters to denote a specific molecular system.

We investigated a number of model molecules (∼20) in a set of preliminary calculations. For this study, we chose systems in which electrostatic alignment is coupled with a steric effect, such as in molecule A. The effect of steric asymmetry is evaluated by varying the size of the substituents 2−4 in molecules A−E. In molecules A−E, the chiral atom (atom 1) and spacer group (atom 2) have partial charges. In A−D, steric asymmetry is created by a large group (atom 3), which we will call "head", and a small strongly attractive group (atom 4), hereafter called "tail". The out-of-plane atom 5 ensures that the molecule is chiral in three dimensions as well as in two dimensions. In molecule E, the headgroup and tailgroup are of the same size. Molecule F is an example of a more complex interacting system. It has four partially charged atoms, as well as a headgroup and a tailgroup.

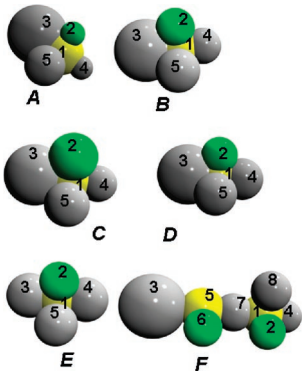

Figure 1. Chiral molecules investigated in this paper. The numbering of atoms is the same as in Table 1, for molecules A−F. As indicated in Table 1, each atom is not necessarily representative of a C, N, O, H, or another actual atom but rather of a particular Lennard-Jones interacting species. The chiral atoms are indicated in yellow, for consistency with the following figures. Atoms colored in yellow and green also carry partial charges. The difference between models A−E is the size of the substituents at the chiral atom. Model F has two chiral centers.

Molecular geometries, indicated by Cartesian atomic coordinates, and the corresponding charges and Lennard-Jones parameters are also included in Table 1. The units are reported scaled by σ_{11} and ϵ_{11} as follows: $\epsilon^*_{ab} = \epsilon_{ab}/\epsilon_{11}$, $\sigma^*_{ab} = \sigma_{ab}/\sigma_{11}$, $U^*_{ab} = U_{ab}/\epsilon_{11}$, $q^* = q\sqrt{1/(4\pi\epsilon_0\epsilon_{11}\sigma_{11})}$, $T^* = k_B T/\epsilon_{11}$. In Table 1, the partial charges are given as fractions of a full electronic charge.

The *xy* plane to which the molecules are restricted in the simulations discussed in this paper, coincides with the molecular *xy* plane, as seen in Table 1. For model A, the effect of this restriction was evaluated in a series of test calculations, in which only the chiral atoms were constrained to a plane, and all other atoms were allowed to move out of plane. Full rotations around *x* or *y* axes are not representative of molecules adsorbed to a surface. To ensure that such moves were not performed in the test calculations, the angle between the 1−5 bond (the bond between atoms 1 and 5) and the *z* axis was restricted to a maximum of 60°. The results of the test simulations were quantitatively similar to the results of the restricted calculations discussed in the results section below.

One further clarification with respect to the nomenclature used in this paper should be made here: We will use the word "racemate" to identify a system being investigated that is macroscopically racemic (50% of each enantiomer). In the adsorbed racemate, local structures can be either chiral or racemic, depending on whether there is local enantiomeric excess in the structure or if the local structure itself is an equimolecular mixture of the two enantiomers. If there are local chiral structures of one handedness, local chiral structures of the opposite handedness are also present, so that the system overall remains macroscopically racemic.

Chiral resolution can be estimated visually from the snapshots included below. To quantify the extent of chiral separation, we calculated average fractions of molecules that have exclusively like and exclusively unlike neighbors (denoted below by F_l and F_u, respectively). As they refer to nearest-neighbors only, F_l and F_u provide a measure of the proportion of molecules involved in homochiral clusters, without contamination from nearby clusters which may be formed of mirror-image molecules. On the other hand, one could define

(57) Neirotti, J. P.; Calvo, F.; Freeman, D. L.; Doll, J. D. *J. Chem. Phys.* **2000**, *112*, 10350.

Table 1. Physical Characteristics of the Racemic Systems Investigated Here[a]

molecule	n_{at}	i	position (x^*, y^*, z^*)	q_i	σ_{ii}^*	ϵ_{ii}^*	molecule	n_{at}	i	position (x^*, y^*, z^*)	q_i^*	σ_{ii}^*	ϵ_{ii}^*
A	5	1	(0,0,0)	0.5	1.0	1.0	D	5	1	(0,0,0)	0.5	1.0	1.0
		2	(0.55,0,0)	−0.5	0.5	1.0			2	(0.61,0,0)	−0.5	0.75	1.0
		3	(0,1.05,0)	0	2.0	1.5			3	(0,1.05,0)	0	2.0	1.5
		4	(0,−0.55,0)	0	0.5	3.5			4	(0,−0.7,0)	0	1.0	3.5
		5	(0,0,0.7)	0	1.0	0.5			5	(0,0,0.7)	0	1.0	0.5
B	5	1	(0,0,0)	0.5	1.0	1.0	E	5	1	(0,0,0)	0.5	1.0	1.0
		2	(0.61,0,0)	−0.5	0.75	1.0			2	(0.61,0,0)	−0.5	0.75	1.0
		3	(0,1.05,0)	0	2.0	1.5			3	(0,0.7,0)	0	1.0	1.5
		4	(0,−0.61,0)	0	0.75	3.5			4	(0,−0.7,0)	0	1.0	3.5
		5	(0,0,0.7)	0	1.0	0.5			5	(0,0,0.7)	0	1.0	0.5
C	5	1	(0,0,0)	0.5	1.0	1.0	F	8	1	(0,0,0)	0.3	1.0	1.0
		2	(0.7,0,0)	−0.5	1.0	1.0			2	(0.55,0,0)	−0.3	0.5	0.7
		3	(0,1.05,0)	0	2.0	1.5			3	(0,2.15,0)	0	2.0	0.25
		4	(0,−0.55,0)	0	0.75	3.5			4	(0,−0.55,0)	0	0.5	3.0
		5	(0,0,0.7)	0	1.0	0.5			5	(0,1.4,0)	0.3	1.0	1.0
									6	(−0.55,1.4,0)	−0.3	0.5	0.7
									7	(0,0.7,0)	0	1.0	0.25
									8	(0,0,0.7)	0	1.0	0.5

[a] n_{at} indicates the number of atoms in a molecule. For each atom, the positions in the molecular reference system (x^*, y^*, z^*), reduced with respect to σ_{11}, partial atomic charges q_i, and reduced Lennard-Jones distance σ_{ii} and strength ϵ_{ii} parameters, are included. For all models, $\sigma_{11} = 1.0$ Å, and $\epsilon_{11} = 10.0$ kJ/mol.

other segregation parameters, which take into account the location and identity of many neighboring molecules. Such parameters would provide information about longer-range homochirality in the system. In the adsorbed structures discussed below, clusters of different handedness are interspersed, and as such, F_l and F_u are the most appropriate choices for quantifying chiral resolution. These fractions were obtained from a series of 2000 snapshots for each temperature, where the snapshots were separated by enough MC moves to allow all molecules to change position. For each molecule in the mixture, two nearest neighbors are found, provided they are within a separation that corresponds to the first minimum in the pair distribution function of the molecular geometric centers. We define the geometric center of the molecule as the point with coordinates $x = \sum_{\text{atoms}} x_i$, $y = \sum_{\text{atoms}} y_i$, and $z = \sum_{\text{atoms}} z_i$.

3. Results and Discussion

3.1. Small (Five-Atom) Model Molecules. Chirality is often thought of as a molecular property. A carbon atom with four different substituents constitutes a chiral atom, and the molecule itself is said to be chiral. The expectation is that this chiral molecule will interact in a way which discriminates between its twin and its enantiomer. Consequently, the interaction potential of a pair of like molecules (a like dimer) is often contrasted with that of a pair of unlike molecules (an unlike dimer) as a measure of the molecule's chirality.[8,9,11,58]

In practice, chirality is relevant not only at the molecular level but in large, multimolecular systems, from which we often attempt to separate the two enantiomers. A given pair of molecules interacts differently in the field of all of the other constituents of the multimolecular system (such as a liquid, a liquid crystal or a solid phase), than when taken in isolation.[59] We discuss in the following paragraphs how chiral recognition changes in this context. The impact of molecular shape and behavior in two or three dimensions will also be considered.

Dimers and Pair Potentials. The pair interaction potential of eq 3 is a function of the separation between the constituent atoms of the two molecules. Because the molecules are rigid, the position of every atom in a molecule is known when the molecular position and orientation, in a given system of coordinates, are known. Consequently, to calculate the intermolecular potential, only the relative position and orientation of the two molecules are needed. We chose to hold one of the molecules fixed and rotate and translate the other. The coordinate system has the geometric center of the fixed molecule as its origin. The range of translations and rotations considered for the second molecule depends on the dimensionality of the problem that is being investigated. For a dimer of nonspherical molecules restricted to two dimensions, there are three degrees of freedom: the intermolecular separation (r^*) taken as the distance between the two geometric centers and two angular degrees of freedom, capturing the relative orientation of the molecules. These are: the azimuthal angle for the position of the geometric center of the second molecule (θ_1) and the rotation of the second molecule around its own z axis (θ_2). In three dimensions, there are five angular degrees of freedom: two describing the position of the intermolecular vector and three describing the orientation of the moving molecule. An interval of $0-2\pi$ was considered for all angles.

To gain some understanding of the type of structures that the molecules would like to form, we calculated the minimum of the interaction potential for a series of values of the intermolecular separation over all values of the angular degrees of freedom. We show in Figure 2a, in black lines, the distance dependence of this interaction potential minimum for like and unlike dimers of molecule A. When the pair is restricted to two-dimensions, like dimers can achieve lower energy configurations than unlike pairs, at separations below 1.5. As the difference in minimum energy between like and unlike dimers is a few times the thermal energy at the temperature of condensation, like configurations are expected to dominate the adsorbed structure at this and lower temperatures.

In the low-density limit the probability of finding a pair of molecules at a given distance, in their minimal energy orientation, is proportional to the function $\gamma(r^*) = e^{-\beta U^*_{\min}(r^*)}$. Figure 2b shows $\gamma(r^*)$, and it can be seen that in this low-density limit, like dimers are one thousand times more likely than unlike dimers at the optimal separation, $r^* \simeq 1.3$.

(58) Gilat, G.; Schulman, L. S. *Chem. Phys. Lett.* **1985**, *121*, 13.
(59) Hansen, J. P.; McDonald, I. R. *Theory of simple liquids*; Academic Press: London, 1976.

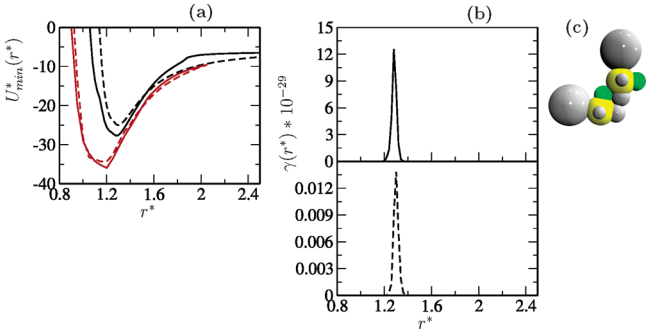

Figure 2. Minimum energies, $U^*_{min}(r^*)$, for like (solid lines) and unlike (dashed lines) dimers of molecule A as a function of intermolecular separation are shown in (a). Black lines correspond to the dimer restricted to two dimensions. Red lines are for the case when three-dimensional degrees of freedom were considered. In (b), the like (solid) and unlike (dashed) low-density limit (not normalized) probability functions, $\gamma(r^*)$, of a dimer of molecule A in two dimensions at $T^* = 0.4$, are presented. The like configuration corresponding to the minimum energy for the two-dimensional case is shown in (c) (the out of plane groups have been shrunk in the snapshot to reveal the chiral atom).

The configuration corresponding to the minimum in $U^*_{min}(r^*)$ or the maximum in $\gamma(r^*)$ for the two-dimensional like dimer is shown in Figure 2c. The structure seen in the figure is the result of the interplay of the three major components of the intermolecular potential: steric repulsion, van der Waals attractions, and electrostatic interactions. The repulsion of the bulky headgroups together with the interaction of the strongly attractive tailgroups lead to the formation of wedge-type structures such as the one seen here. Dipolar alignment provides the additional directional preference of the dimer. In fact, dipolar alignment is not completely satisfied here, as dipoles are most favorably aligned in antiparallel configurations, but there is a competition between this and the other components of the intermolecular potential that has as an outcome the present minimum structure. At first glance, the intermolecular potential composed of a Lennard-Jones and an electrostatic component is simple enough. Complexity results from the fact that molecules have anisotropic shapes. The cumulative interaction of all the atomic components leads to complex behavior even in the case of a dimer. As will be shown below, the behavior of multibody systems of such molecules is significantly more complex.

Multimolecular Assembly of A Racemates in Two Dimensions. We now consider the results of two-dimensional simulations of a racemic cluster of 100 molecules of type A. The adsorbed structure at low temperatures, shown in Figure 3a, is the result of the optimal geometry seen in Figure 2c. When more than two molecules are available, the dimer minimum potential structure becomes a building block for small clusters of like molecules. The rosette-type micellar structures formed on the surface are themselves chiral and are characterized by opposite alignment directionality for the two enantiomeric forms. These structures resemble in geometry those obtained experimentally from 1-nitronaphthalene,[35,60] trimesic acid by complexation on the surface with Fe,[20,61] oligo-(*p*-phenylenevinylene),[18] and rubrene.[29] The interactions involved in structure formation in these experimental systems are much more complex than in our

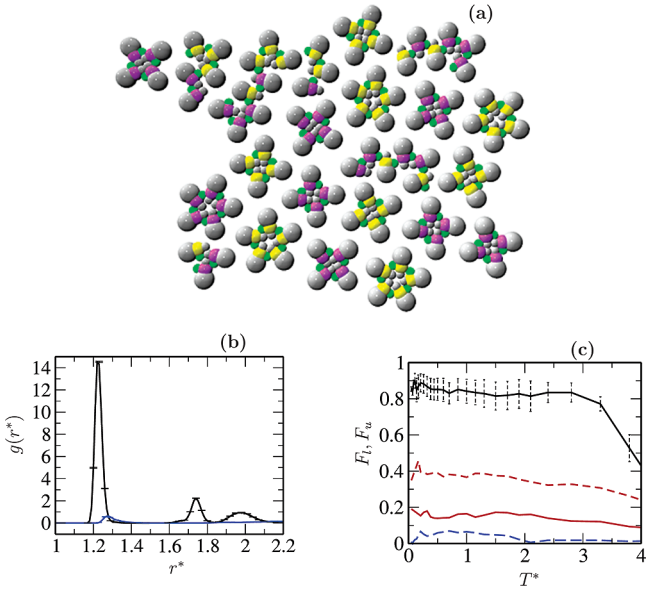

Figure 3. Simulation snapshot for a 100 molecule racemate of molecule A at $T^* = 0.4$, (a). Although identical, the central atoms in the two enantiomers were indicated in yellow and purple, respectively, for the clarity of the image. In each molecule, the fifth atom (Figure 1) is positioned below the chiral atom and is therefore not seen in the picture. The like (black line) and unlike (blue line) pair distribution functions of the geometric centers are shown in (b). The fraction of molecules with exclusively like neighbors (F_l, solid lines) and with exclusively unlike neighbors (F_u, dashed lines) are shown in (c) for two-dimensional (black and blue lines) and three-dimensional (red lines) calculations. Error bars in (b) and (c) are calculated as standard deviations from the average over the course of a simulation run.

simple models, and the geometry of the substrate is expected to have a strong impact on the adsorbed structure. Nevertheless, our results suggest that the basic physics for the formation of the rosette chiral aggregates in the experimental systems may be due to the optimal interaction between a pair of like molecules.

Micellar assembly for molecules of type A is driven by the asymmetry of the Lennard-Jones component of the intermolecular potential. The small attractive tailgroups gather in the center of the cluster, whereas the bulky, less attractive headgroups are pushed to the exterior of the micelle. On the other hand, Lennard-Jones interactions alone do not lead to chiral separation. In a simulation of similar molecules, without partial charges, racemic micelles were obtained. The alignment within the micelles, and thus chiral recognition, is induced by the additional electrostatic component of the potential, showing the need to have steric, van der Waals and directional (electrostatic) interactions for chiral recognition.

The structure in the racemate of Figure 3a can be characterized by the pair distribution function of the molecular geometric centers ($g(r^*)$) as shown in Figure 3b. The dominant feature is the sharp probability of like configurations at about $r^* = 1.2$, which is topologically similar to the peak in $\gamma(r^*)$ displayed in Figure 2b. However, the multimolecular character of the aggregates is manifested in $g(r^*)$ in a few ways. First, the peak at small separations, denoting near neighbors, is not as sharp as the one obtained from the intermolecular interactions through $\gamma(r^*)$. Second, the presence of additional peaks in the pair distribution functions shown in Figure 3b shows the aggregation into clusters. Third, the probability of unlike pairs, as seen in the unlike pair distribution function, is 1 order of magnitude

(60) Böhringer, M.; Schneider, W.-D.; Berndt, R. *Angew. Chem., Int. Ed.* **2000**, *39*, 792.
(61) Messina, P.; Dmitriev, A.; Lin, N.; Spillmann, H.; Abel, M.; Barth, J. V.; Kern, K. *J. Am. Chem. Soc.* **2002**, *124*, 14000.

smaller than that of like configurations. This is to be compared with the 3 orders of magnitude that can be deduced from the intermolecular pair interactions, as shown in Figure 2b.

To quantify the extent of chiral separation, we calculated the fraction of molecules with exclusively like and exclusively unlike neighbors. In two-dimensional racemates of molecule A, about 80−90% of molecules have exclusively like neighbors, at temperatures lower than $T^* = 3$, as seen in Figure 3c. The homochiral clusters formed on the surface are mostly four-molecule clusters (about 60%), with some five-molecule and some three-molecule clusters also present.

Comparison with Three-Dimensional Simulations. To understand the importance of the restriction to two dimensions in the formation of chirally segregated clusters, we also investigated the behavior of molecule A when allowed to evolve in three dimensions. The three-dimensional pair potential for like and unlike dimers of A is included in Figure 2a (red lines). When three-dimensional degrees of freedom are considered, lower minima are obtained for the interaction potential of like and unlike pairs at all separations for which $r^* > 2$. This is expected because the two-dimensional degrees of freedom are a subset of the three-dimensional variables. For both like and unlike dimers, the optimal geometries obtained in three dimensions are wedge structures similar to those shown in Figure 2c. Because the molecules are no longer restricted to a certain surface binding position, they are able to achieve antiparallel dipolar configurations, with dipoles oriented perpendicular to the wedge plane. The difference between the energies of these optimal structures is much smaller in the three-dimensional case than in two dimensions. The origin of this difference resides in the fact that atom 5 induces some steric strain in the unlike dimer and can be much better accommodated in the like dimer. The potential difference, although relatively small, leads to higher $\gamma(r^*)$ probability values for the like than for the unlike configurations.

On the other hand, simulation results indicate that chiral resolution is not achieved when the molecules are allowed to equilibrate in three dimensions. We only included here the fraction of molecules with like and unlike neighbors (red curves in Figure 3c), which show that molecules are more likely to be found close to their enantiomers. In fact, examination of snapshots, not included here, reveals that micellar formation occurs in the three-dimensional case as well, but that the 8−10 molecular three-dimensional micelles are locally racemic. The stability of the optimal homochiral geometry of the isolated dimer is overcome by multibody interactions leading to micellar formation in three dimensions. Chiral segregation in the case of racemates of molecule A is thus a direct consequence of the restriction to two dimensions. Restriction of molecular degrees of freedom promotes separation through aggregation in two-dimensional micelles, where the like molecules are found at the optimal angular arrangement.

Molecular Shape and Chiral Resolutions. The impact of substitution at the chiral group on the quality of chiral segregation upon adsorption is illustrated in Figures 4 and 5. In molecule A, both the spacer and the tailgroup are small, half of the size of the chiral group, compared to the size of the headgroup. The chiral rosette clusters formed on the surface are consequently small, but the quality of resolution is high. As the size of the spacer and the tailgroup increases, some larger clusters form on the surface (mostly five-molecular clusters, but also some six- to eight-molecule ones), but the quality of the separation is progressively lost. Good resolution is achieved in racemates B and C, where more than 80% of molecules have exclusively like neighbors at low and intermediate temperatures, as seen in Figure 5. In racemate D, where the tailgroup is more bulky and closer in size to the headgroup, the quality of the resolution is significantly lower, see Figure 4c. As shown in Figure 5, only about 60% of molecules have exclusively like neighbors in this case. Here, molecules tend to form like chains rather than micellar structures, because of the reduced steric asymmetry of the molecules.

Finally, in the case of racemate E, the headgroup is smaller in size than in the other models. In this case, molecules can accommodate a larger number of neighbors in close proximity, and equilibrium is achieved in a compact geometry such as the one shown in Figure 4d, with local chain structures and no chiral segregation. The progressive loss of chiral separation when molecular asymmetry is reduced is an illustration of the important role of steric interactions, or molecular shape, on the interplay of factors that enables chiral separation, demonstrating that electrostatic interactions by themselves are not enough to promote separation. It is the interplay between all the interactions that governs separation.

From Figure 5 we see that F_l can be used as an order parameter for micellar aggregate formation in these systems. At high temperatures, $F_l \simeq F_u$ and both are small, because the systems are in the two-dimensional gas phase and any associations of molecules are random events. As the temperature decreases, a transition to chiral micellar aggregates may occur. For those compounds that form micellar aggregates, large values of F_l are observed at low and intermediate temperatures. We show in the Supporting Information the heat capacity dependence on temperature for a racemate of type B, where the same temperature range of about $T^* = 3$ is found for micellization.

3.2. Molecules with Two Chiral Centers. We investigated chiral resolution in molecules that possess two chiral centers. For this, we performed calculations on 100 and 200 molecule systems, in two and three dimensions, for a racemate of molecule F. We include in Figure 6 a snapshot of the 200-molecule racemate for this model, which shows chiral resolution, with ten-molecule chiral clusters, in structures which again resemble micellar aggregates. A competition between the formation of like micellar clusters and locally racemic double chain structures such as the one identified with a blue oval, is also observed from the figure. From analysis of the relationship between the pair potential and the simulated structures obtained in the adlayer, it becomes apparent that the formation of chiral micellar structures for molecule F occurs through a different mechanism than that discussed above for molecule A.

Effective Pair Interactions. In Figure 7, we contrast the potential and probability functions for isolated pairs of like or unlike molecules of type F with the potential of mean-force and the pair distribution functions for the 200 molecule racemate simulated here. The minimum values of the energy for all relative orientations of the pair of molecules, $U^*_{min}(r^*)$, for like and unlike dimers of type F, are plotted as a function of intermolecular separation in Figure 7a. It can be seen from the figure that heterochiral dimers can achieve a lower energy configuration than the optimal structure of the homochiral dimer

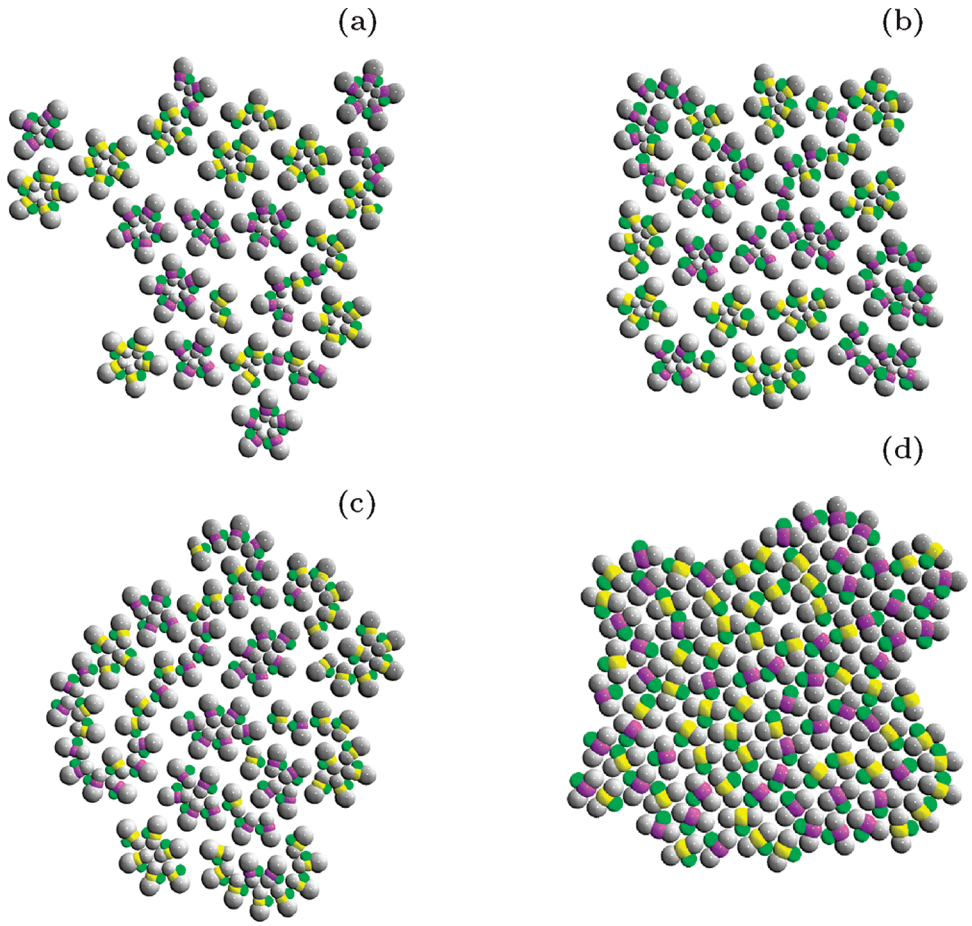

Figure 4. Low temperature, $T^* = 0.1$, simulation snapshots for racemates of molecules B−E ((a−d), respectively). Although identical, the central atoms in the two enantiomers were indicated in yellow and purple, respectively, for the clarity of the image. In each molecule, the fifth atom (Figure 1) is positioned below the chiral atom, and is therefore not seen in the picture. The difference in substituent sizes at the chiral atom leads to different types of adsorbed monolayers.

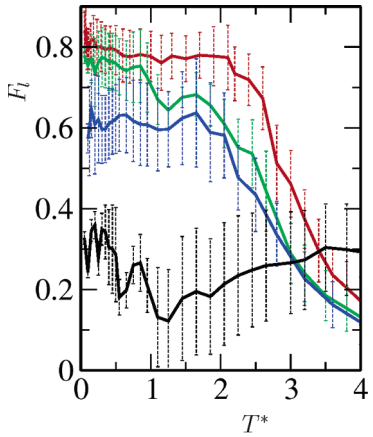

Figure 5. Temperature dependence of the fraction of the total number of molecules involved in like local structures. Red, green, blue, and black lines represent racemates of molecules B, C, D, and E, respectively. Error bars indicated standard deviations from the average.

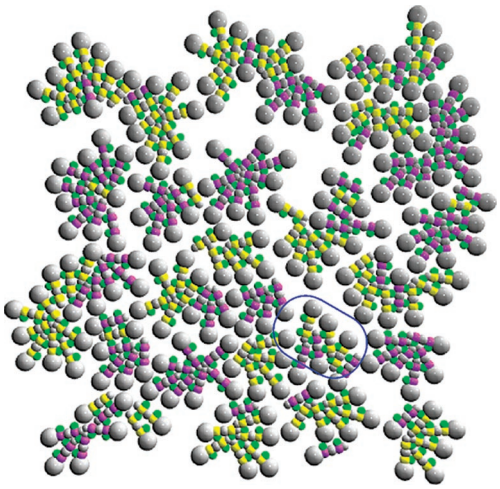

Figure 6. Simulation snapshot of a 200 particle racemic system of molecule F at $T^* = 0.7$. The blue oval indicates an example of a double chain heterochiral structure competing with segregated homochiral clusters on the surface.

(at $r^* = 1.31$). The minimal energies for unlike clusters are lower than those for like clusters for a limited interval, between 1.2 and 1.6. In contrast, the plot of homochiral dimer energies has a very broad well, with some local structure. In other words, like dimers can achieve similar minimum energies for a large interval of intermolecular separations. The multidimensional surfaces of homo- and heterochiral energies are significantly more complex in the case of molecule F than the ones discussed in the previous section for molecule A. Contour plots of the angular dependence of the dimer potential energies, at a few representative values of the intermolecular separation, are shown in Figure 8. Snapshots of the configuration corresponding to the minimum on each plot are also included in the figure. The contour surfaces provide direct information about the relation-

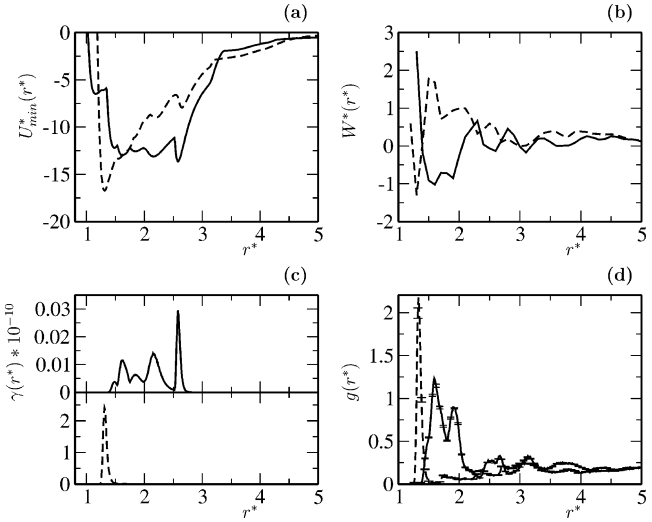

Figure 7. Minimum energies, $U^*_{min}(r^*)$, for like and unlike dimers of molecule F as a function of intermolecular separation are shown in (a). Low-density limit probabilities, $\gamma(r^*)$, corresponding to $U^*_{min}(r^*)$, are shown in (c). $U^*_{min}(r^*)$ and $\gamma(r^*)$ are calculated for isolated pairs of molecules. Solid and dashed lines represent like and unlike dimers, respectively. The results of the multimolecular simulations are shown in (b) and (d). In (d), like (solid) and unlike (dashed) pair distribution functions of the geometric center, $g(r^*)$, for racemate F at $T^* = 0.7$, are presented. The like (solid) and unlike (dashed) potentials of mean force, $W^*(r^*)$, are shown in (b).

ship between the relative orientation of the two molecules and their interaction potential. We show contours corresponding to minima in Figure 7a: $r^* = 1.31$, 2.15, and 2.58.

From the contour plots, the multidimensional pair potential is repulsive over large angular domains at small separations (Figure 8a and b), with deep narrow attractive wells at antiparallel configurations for both like and unlike dimers. In other words, there is a very limited interval of dimer orientations for which the potential is attractive. All other orientations are high in energy due to steric repulsion. Because of the steric hindrance of the bulky headgroup, at these separations dimers prefer antiparallel structures as seen in Figures 8a and b. The dipolar alignment in this configuration is repulsive for like dimers and strongly attractive for unlike dimers, which are therefore more stable.

The topology of the surface at short separations, largely repulsive, with narrow wells, indicates that phases in which such configurations dominate would be strongly ordered, compact phases, such as solid or smectic phases. At larger separations, illustrated by Figure 8c−f, the steric hindrance is reduced, and thus, the Lennard-Jones component of the intermolecular potential is attractive over a large range of relative orientations. At the same time, the relative strength of the Coulomb interaction decreases because the molecular dipoles are further apart. The surface of intermolecular interactions at these separations is largely attractive, with shallower minima. At these intermolecular distances a large range of relative orientations have similar energies. There is a large degree of in-plane isoenergetic rotational freedom in this region. Homochiral pairs are more stable at these separations because of the better dipolar alignment for like than for unlike dimers, as illustrated in the dimer configurations.

Multimolecular Assembly Mechanism. The like and unlike pair distribution functions, $g(r^*)$, and potential of mean force, $W^*(r^*)$, at $T^* = 0.7$ for the 200 molecule racemate are shown in Figure 7d and b, respectively. The potential of mean force is the effective interaction potential between two particles averaged over all the configurations of the other molecules. This quantity is determined from the pair distribution function: $-\beta W^*(r^*) \propto \ln g(r^*)$.[62] The significant difference between Figure 7a and b is due to two effects. First, the presence of the other molecules in the fluid impacts the interaction between the two molecules at a given separation r^* (a multibody effect). The second effect is that the interaction shown in Figure 7a is calculated between a pair of molecules that are in a specific orientation, which minimizes the pair potential. Other orientations are not represented in the shown values of $U^*_{min}(r^*)$. The potential of mean force, on the other hand, corresponds to an average over all allowed orientations and configurations in the fluid.

The importance of the difference between the intermolecular potential and the potential of mean force is as follows. The pair potential for molecule F would lead us to predict that a multimolecular racemic collection of these types of molecules would not segregate in two dimensions, because heterochiral pairs are more stable than homochiral pairs. On the other hand, simulation results illustrated by $g(r^*)$ and the snapshot in Figure 6 show that the system segregates at the temperatures investigated here. There are two factors that contribute to chiral symmetry breaking in the 200 molecule racemate: the multibody potential and entropy. Although, when taken in isolation, an unlike dimer is significantly more stable than a like dimer, in the condensed phase, molecules form multibody aggregates rather than dimers. In a circular micelle, such as the ones seen in Figure 6, a molecule interacts attractively with its nearest and next-nearest neighbors and so on. This also happens in double-chain heterochiral structures, but the multibody interaction of the strongly attractive tailgroups is favored in the micellar structure. To evaluate the relative magnitude of different effects in structure formation, we compared the potential difference between a randomly selected 8 molecule homochiral micelle in one of the snapshots, and a perfectly aligned 8 molecule double chain racemic structure. The double chain structure is still lower in energy, but only by about an amount per molecule roughly equal to the thermal energy. This energy difference can be overcome entropically by the many different ways that the molecules can pack in the aggregates and the ability of the molecules in the aggregates to have the same energy in a relatively large range of distances, see Figure 7a.

Entropy favors homochiral structures in this system through mixing of the two types of chiral micelles (a minor contribution) and through a configurational entropy contribution. Unlike low-energy structures can be obtained in a very limited range of pair geometries, as shown by the deep narrow unlike wells in Figures 7a and 8b. On the other hand, a large range of like pair geometries have similar energies, as discussed above. This relative configurational freedom of like pairs implies that configurational entropy will be significantly more favorable for like structure formation.

An alternative illustration of these conclusions is provided by the pair distribution function. In the low-density limit, the probability of pairs of molecules in optimal configurations is

(62) Strictly speaking, $\beta W^*(r^*) = -\ln g(r^*)$.[59] Because of the finite size of the systems investigated here, the long range value of $g(r^*)$ is not one. To renormalize the long-range behavior of $W^*(r^*)$, we use the modified equation $\beta W^*(r^*) = -\ln g(r^*) - 1$ in this paper.

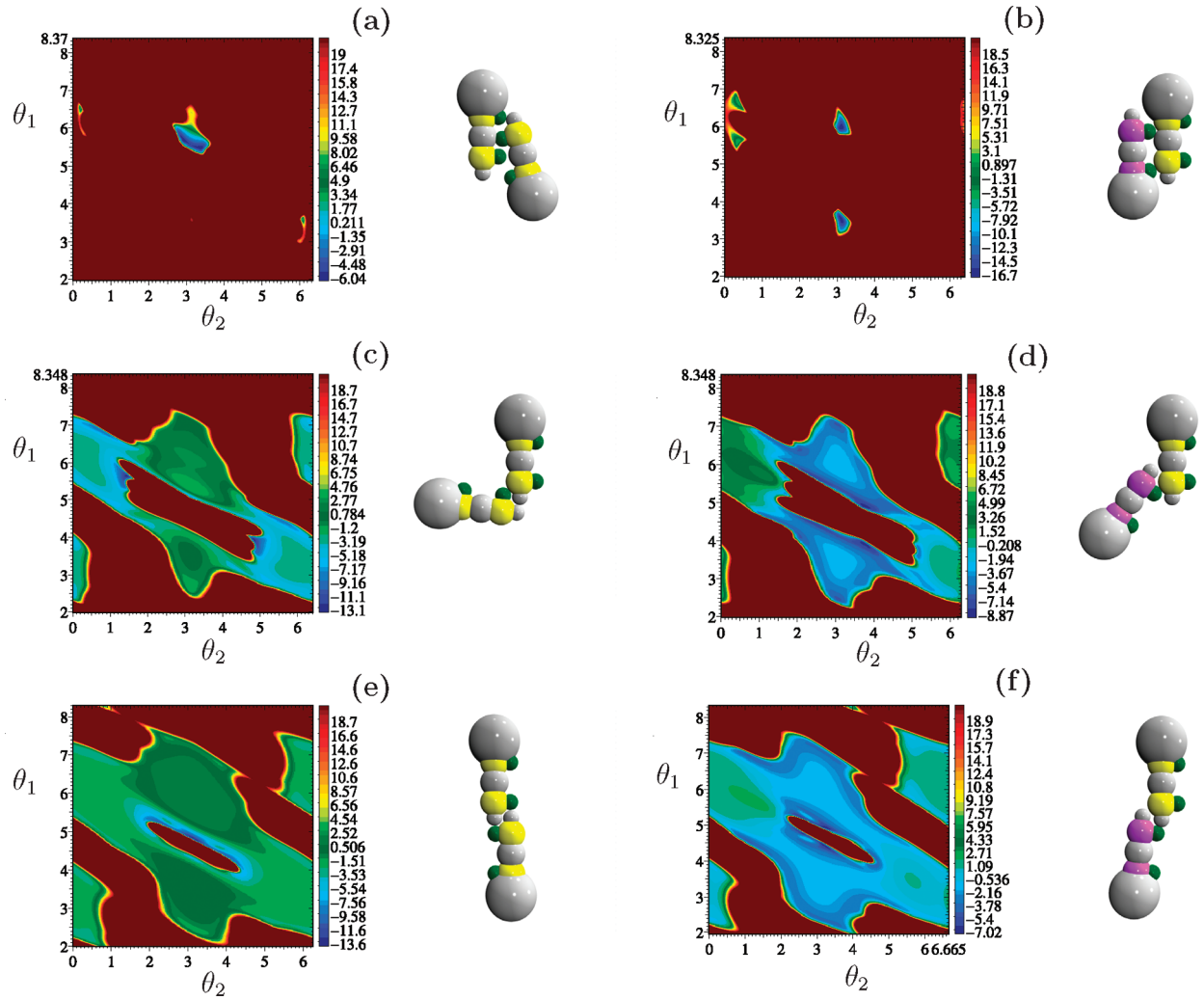

Figure 8. Potential energy surface (units of ϵ_{11}) for like ((a), (c), and (e)) and unlike ((b), (d), and (f)) dimers of molecule F, at constant intermolecular separation r^*. In (a)/(b), (c)/(d), and (e)/(f), $r^* = 1.31$, 2.15, and 2.58, respectively. θ_1 is the azimuthal angle of the position vector of the second molecule (this vector has size r^*). θ_2 is the rotation angle of the molecule around its geometric center. Both angles are expressed in radians. At $\theta_1 = \theta_2 = 0$, the two molecules are parallel and r is along the x axis. The minimum energy configuration corresponding to each contour plot is presented to the right of the contour.

proportional to $\gamma(r^*)$, shown in Figure 7c. This is equivalent to the low-density pair distribution function calculated for that optimal relative orientation, and is determined exclusively by the minimum pair potential. If we consider the two interacting particles in the configurations corresponding to potential energy minima, the resulting $\gamma(r^*)$ is very large for unlike pairs and relatively negligible for like pairs. Instead, our simulations at finite densities reveal the pair distribution functions shown in Figure 7d, with a large probability of heterochiral pairs at very small separations ($r^* < 1.3$), whereas the range of intermediate separations is dominated by homochiral structures. The differences between the two functions can be explained based on the same arguments used to interpret the energetic functions discussed above.

4. Conclusions

In this paper, we investigate chiral symmetry breaking in macroscopically racemic systems, when constrained to assemble in two dimensions. Chiral recognition occurs when, locally, the preferential orientation of groups of like molecules is achieved via electrostatic or steric alignment. A surface can facilitate this preferential alignment by limiting the configurational space available to the racemate.

We examine a number of model systems by using a parallel tempering Monte Carlo technique and restricting the racemate to assemble in two dimensions. We find that by controlling the balance between steric and electrostatic interactions, one can direct the assembly toward formation of small aggregates of identical molecules. The models investigated here have steric asymmetry due to the presence of a bulky headgroup and a small, strongly attractive tailgroup. This molecular geometry conditions assembly in small four- to ten-molecule micellar clusters. When the molecular shape asymmetry is complemented by dipolar alignment, chiral rosette clusters of three to seven like molecules are assembled on the surface. Dipolar alignment within the micelle provides selectivity for formation of homochiral structures. This alignment also accounts for the chirality of the resulting structure. At the same time, three-dimensional simulations of the same racemates show racemic micelle formation which indicates that chiral separation is directly determined by adsorption (or, in this case, constraint to two-dimensional assembly). The self-assembled structures obtained

in this study resemble rosette clusters observed experimentally[18,20,39] for adsorption of racemates on solid surfaces.

Two types of configurations compete in structure formation in our racemic systems. Chiral rosette clusters of like molecules are seen to coexist with locally racemic double chains in which unlike molecules alternate. The building blocks for the two types of structures can be obtained by examination of the pair potentials for like and unlike dimers. Like dimers form wedge-type structures, in which the strongly attractive tailgroups are close by and dipoles are (loosely) aligned, or linear configurations, in which the headgroups are again together and dipoles are antiparallel. Unlike dimers are optimally arranged in antiparallel configurations, also with aligned dipoles and tailgroups further apart. Depending on the molecular structure, one or the other dimer geometry is more stable. Nevertheless, we show that examination of the pair potential for the two types of dimers is insufficient to predict the outcome of this competition in the assembled adlayer.

For some of the smaller models considered here, like pairs are more stable and the optimum dimer structure becomes a building block in chiral micelle formation in the condensed adsorbed phase. On the other hand, in condensed phases, molecules interact through pair and multibody potentials. For all of the systems investigated here, multibody interactions favored the formation of micellar structures. In these geometries, the strongly attractive tailgroups of as many as 10 molecules can group together in the center of the micelle, whereas the bulky headgroup is expelled toward the exterior of the micelle. This effect is particularly important in the case of molecule F, for which unlike pairs are significantly more stable than like pairs and consideration of pair potentials alone would lead to the prediction of a locally racemic adsorbed phase. On the contrary, because of the multibody effect described here and the configurational entropy arising from the shallow potential that also favors formation of homochiral aggregates, these types of structures are seen to dominate the adsorbed phase. Specifically, homochiral configurations are entropically favored because there is a larger range of distances and angles that optimize formation of these types of aggregates. The favoring of homochiral clusters is indicated by the potentials of mean force, which show greater stability for the effective like than unlike interactions, in sharp contrast to the simple pair potentials. It will be interesting to investigate further the conditions under which the balance between like and unlike configurations can be slanted toward exclusive formation of chiral local structures.

In chiral separations at the solid surface, a complex set of effects cooperate to yield the final adsorbed pattern. An understanding of the individual effects of these factors could enable us to control the process and predict the relationships between molecular structure, molecular environment, and chiral resolution. Here, we investigated whether the simple restriction to two-dimensionality can be a basis for chiral symmetry breaking in systems that are macroscopically racemic. The next steps in understanding chiral separations at adsorption should be the consideration of solvent effects, the geometric and energetic makeup of the underlying substrate, and the study of the role of dynamic effects such as diffusion.

Acknowledgment. I.P. and M.A.R. are grateful to the MURI program of the DoD for support of this work. They also thank the NSF-MRSEC program, for support through the Northwestern MRSEC, and the chemistry division of the NSF. I.S. acknowledges partial support from the NSF. This research was performed in part using the Molecular Science Computing Facility (MSCF) in the William R. Wiley Environmental Molecular Sciences Laboratory, a national scientific user facility sponsored by the U.S. Department of Energy's Office of Biological and Environmental Research and located at the Pacific Northwest National Laboratory, operated for the Department of Energy by Battelle.

Supporting Information Available: Temperature dependence of heat capacities and illustrative snapshots. This information is available free of charge via the Internet at http://pubs.acs.org.

JA066422B